Adaptive EWMA-S^2 Control Charts with Time-Varying Smoothing Parameter

Willy Ugaz^{a}*, Andrés M. Alonso^{b,c}†, Ismael Sánchez^{a,b,c}‡

^{a} Department of Industrial Engineering and Systems, Universidad de Piura

^{b} Department of Statistics, Universidad Carlos III de Madrid

^{c} Instituto Flores de Lemus, Universidad Carlos III de Madrid

Abstract

Memory charts like EWMA-S^2 or CUSUM-S^2 can be designed to be optimal to detect a specific shift in the process variance. However, this feature could be a serious inconvenience since, for instance, if the charts are designed to detect small shift, then, they can be inefficient to detect moderate or large shifts. In the literature, several alternatives have been proposed to overcome this limitation, like the use of control charts with variable parameters or adaptive control charts. This paper proposes new adaptive EWMA control charts for the dispersion (AEWMA-S^2) based on a time-varying smoothing parameter that takes into account the potential misadjustment in the process variance. The obtained control charts can be interpreted as a combination of EWMA control charts designed to be efficient for different shift values. Markov chain procedures are established to analyze and design the proposed charts. Comparisons with other adaptive and traditional control charts show the advantages of the proposals.

Keywords: Adaptive control charts, Average Run Length, EWMA, CUSUM, Statistical Process Control.

---

*Corresponding author. Department of Industrial Engineering and Systems; Universidad de Piura; Calle Mártir José Olaya 162, Miraflores, Lima, Perú. email: willy.ugaz@udep.pe.

†Department of Statistics and Instituto Flores de Lemus; Universidad Carlos III de Madrid; Calle Madrid 126, 28903, Getafe, Madrid, Spain. email: amalonso@est-econ.uc3m.es.

‡Department of Statistics and Instituto Flores de Lemus; Universidad Carlos III de Madrid; Avd. de la Universidad 30, 28911, Leganés, Madrid, Spain. Department of Industrial Engineering and Systems; Universidad de Piura; Calle Ramón Mugica 131, Piura, Perú. email: ismael@est-econ.uc3m.es.

1 Introduction

The use of control charts as a process monitoring tool has become increasingly popular in the field of statistical process control (SPC). Shewhart control charts (Shewhart, 1931) can be used for monitoring the mean or the variability of the process. In many practical applications, it is even more important to control shifts in the process variability rather than the mean, since an increase of the variability process causes an increased number of defective products while a decrease of process variability implies an improvement of process capability (Acosta-Mejia et al., 1999). Besides, it is meaningless to claim a shift of the process mean unless it is sure that the process variability is in control.

Shewhart control charts such as the range R or the unbiased sample variance S^2 control charts can be used for monitoring the variability of rational subgroups sampled of the process. However, as in the case of monitoring the process mean, these procedures are not very sensitive to small shifts.

In order to increase the sensitivity to small shifts, the literature has proposed some alternative procedures that use statistics with memory, usually called memory control charts or time-weighted control charts. It is known that the most popular memory control charts are the CUSUM and the EWMA charts, which have been recognized as potentially powerful tools in quality control. One of the first CUSUM control charts for monitoring variability was introduced by Page (1963) and then studied by Bagshaw and Johnson (1975), Hawkins (1981), Box and Ramírez (1991a,b,c), Chang and Gan (1995), Castagliola et al. (2009) and Nazir et al. (2015), among others.

Furthermore, Wortham and Ring (1971), Sweet (1986) and Ng and Case (1989) investigated the properties of EWMA control charts for monitoring the process variability but they were not able to introduce formal design strategies for the problem. Box, Hunter and Hunter (1978), among others, introduced the use of the logarithm of the sample variances since it is more approximately normally distributed than the sample variance by itself. Crowder and Hamilton (1992) proposed an EWMA control chart for monitoring the variability based on the logarithmic transformation of the sample variance, $\log\left(S^2\right)$, due to its simplicity and efficiency. Castagliola (2005) proposed a bilateral EWMA control chart for monitoring the variability using a logarithmic transformation of three parameters (a particular case of the Johnson, 1949 transformations) to improve normality.

As an extension of the Crowder and Hamilton (1992) proposal, Shu and Jiang (2008) presented an EWMA control chart for monitoring the variability (NEWMA), which truncates the negative normalized observations to zero in the statistical traditional EWMA. Maravelakis and Castagliola (2009) propose a modified EWMA control chart for monitoring the standard deviation when the parameters are estimated. Castagliola et al. (2010) presented an EWMA control chart that improves the 2005 version. This chart uses the Johnson transformation of four parameters to attain normality.

Other interesting researches that study CUSUM and EWMA control charts for the process variability can be found in Tuprah and Ncube (1987), MacGregor and Harris (1993), Gan (1995), Lowry et al. (1995), Acosta-Mejia (1998), Amin et al. (1999), Chao-Wen and Reynolds (1999), Acosta-Mejía et al. (1999), Huwang et al. (2010), Abbasi (2010), Abbasi and Miller (2013) and Haq et al. (2014), among others.

Analogously to the control of the process mean, adaptive CUSUM and EWMA control charts for monitoring the variability process can be proposed based on time-varying versions of the parameters that control the memory of the charts; that is k in CUSUM charts and λ in EWMA charts. By adapting the memory, we can make charts sensitive to both small and large shifts. The intuition behind these adaptive charts is to use a measure of the potential presence of a shift. Accordingly, the value of the parameter is increased when it is suspected that the process could be out of control due to a large shift. Conversely, if the data show strong evidence of being in control or with a small shift, the parameters tend to be smaller, easing the detection of potential small shifts. This kind of adaptation scheme is the one we pursue in this paper.

Shu et al. (2010) proposed an adaptive CUSUM control chart for monitoring shifts in the process variability (ACUSUM-S^2). This chart is an extension of the ACUSUM control chart for monitoring the process mean initially proposed by Sparks (2000). This ACUSUM-S^2 chart dynamically adjusts its reference value according to a current estimate of the process variance and does not require precise information about the magnitude of shift.

Capizzi and Masarotto (2003) developed an AEWMA control chart for monitoring the process mean based on weighting recent observations using an score function of the current error $e_t = x_t - y_{t-1}$, where x_t is the last observation of the process and y_{t-1} is the previous value of the monitoring statistic. In particular, if e_t is small, the value of λ tends to be small, like in conventional EWMA chart, since the process seems to be in control. However, if e_t is large the value of λ tends to be large, since the risk of being out of control is higher.

Shu (2008), considering the statistic of Crowder and Hamilton (1992), proposed an adaptive EWMA control chart for monitoring the process variability. This chart is based on the latest observations dynamically weighted according to an appropriate function of the current prediction error. It is actually an extension of Capizzi and Masarotto (2003) for monitoring the process mean.

Additionally, some new AEWMA control charts for monitoring the process mean are proposed by Ugaz et al. (2017). These charts use specific statistics that quantify the evidence of a shift from data, that is, statistics based on the distance from observations x_t to the process mean μ_0 or based on the prediction error, e_t, or just based on the level of y_{t-1}. Subsequently, the statistics are translated to

time varying smoothing factor λ_t. Those AEWMA control charts are competitive with respect to the proposal of Capizzi and Masarotto (2003).

In this paper, considering the proposals of Ugaz et al. (2017), some alternative AEWMA-S^2 control charts are proposed. To that aim, several measures of the potential shift of the process variance are suggested. For each measure of potential shift, alternative methods to translate such measure into a time varying smoothing factor are discussed. Procedures to compute the ARL of the proposed AEWMA-S^2 based on Markov chain approximations are obtained, which allow us to attain the optimal designs. A numerical comparison of these alternative approaches and some alternatives in the literature is presented.

The rest of the article is organized as follows. In Section 2, the notion of the adaptive EWMA-S^2 control chart is introduced. In Section 3, AEWMA-S^2 control charts with time varying λ_t based on the last observation are proposed. In Section 4, AEWMA-S^2 control charts with time varying λ_t based on the level of the control statistics are proposed. Section 5, presents the results of several comparisons between alternative control charts and the proposed AEWMA-S^2 control charts. Finally, in Section 6, some concluding remarks are given.

2 Adaptive EWMA-S^2 control chart

Assume that observations $X_{t,i}$, $t = 1, 2, \cdots$ and $i = 1, 2, \cdots, n$ are independent and identically distributed following a normal distribution $N\left(\mu, \sigma_t^2\right)$. Furthermore, we are mainly interested in detecting increases in the process variance, i. e., $\sigma_t^2 = \sigma_0^2, t < t^*$ and $\sigma_t^2 > \sigma_0^2, t \geq t^*$ and $\tau_t = \sigma_t/\sigma_0$. Let S_t^2 be the variance of the $t-$th rational subgroup of size n defined by $S_t^2 = (1/(n-1)) \sum_{i=1}^{n} \left(X_{t,i} - \overline{X}_t\right)^2$, where $X_{t,i}$ is the $i-$th observation of the $t-$th rational subgroup and $\overline{X}_t$ is the $t-$th subgroup mean. Crowder and Hamilton (1992) suggested the EWMA chart for monitoring increases in the process variance with the statistic,

$$y_t = \max\left[0, \lambda M_t + (1 - \lambda) y_{t-1}\right], \quad y_0 = 0, \tag{1}$$

where $M_t = \ln\left(S_t^2/\sigma_0^2\right)$, which is approximately normal distributed (Shu and Jiang, 2008). The mean and variance of the transformed variable M_t are approximated by,

$$\mu_{M_t} = \ln\left(\tau_t^2\right) - \frac{1}{n-1} - \frac{1}{3(n-1)^2} + \frac{2}{15(n-1)^4}, \tag{2}$$

and

$$\sigma_{M_t}^2 = \frac{2}{n-1} + \frac{2}{(n-1)^2} + \frac{4}{3(n-1)^3} - \frac{16}{15(n-1)^5}, \tag{3}$$

4

respectively. It is important to note that $\sigma^2_{M_t}$ only depends on n. Because of that M_t can be monitored as X_t in the EWMA chart for monitoring the process mean. This EWMA-S^2 control chart signals when,

$$y_t > h, \qquad (4)$$

where h is a threshold that determines the in control average run length (ARL$_0$).

To design the EWMA-S^2 control chart for the variance process, the parameter values of λ and h for some rational subgroup of size n must be selected. λ and h, which are defined in (1) and (4) can be chosen in such a way that the chart is optimal for detecting a prespecified shift in the variance process for a given ARL$_0$. The influence of the design parameters in the performance of the EWMA-S^2 has been studied by Box, Hunter and Hunter (1978), Crowder and Hamilton (1992), Castagliola (2005), Shu and Jiang (2008), Castagliola et al. (2010), Huwang et al. (2010), Abbasi (2010), among others.

The ARL of this AEWMA-S^2 is a function of the shift, $\tau = \sigma_1/\sigma_0$ (σ_0 is the standard deviation of the in control process and σ_1 is the standard deviation of process when it is out of control), λ, h and n. It can be written as ARL=ARL($\lambda, h|\tau, n$). Then, by solving the following optimization problem, the optimal values of λ and h that minimize the ARL($\lambda, h|\tau, n$) can be obtained:

$$\min_{\lambda, h} \left(ARL\left(\lambda, h|\tau, n \right) \right)$$

subject to:

$$ARL\left(\lambda, h|\tau = 1, n \right) = ARL_0,$$

The $ARL\left(\lambda, h|\tau \neq 1, n \right)$ can be approximated by a discrete Markov chain procedure (see, for instance, Brook and Evans, 1972 or Lucas and Saccucci, 1990).

Whereas an optimal EWMA-S^2 chart would need a different value of λ for each τ, the same value of λ can be a reasonable option for some range of shifts. However, there is not a single value of λ that can provide optimal or nearly optimal EWMA charts for both small and large values of τ. To illustrate this finding, we have calculated the optimal pair (λ, h) denoted as (λ^*, h^*) for each shift $\tau \in [1, 3]$, for ARL$_0 = 200$ and $n = 5$, using the proposal of Crowder and Hamilton (1992) with the transformation M_t. The corresponding minimum ARL is denoted as ARL*; that is ARL$^* =$ARL(λ^*, h^*, τ) . Figure 1 and Table 1 show the values of λ^* for each τ as well as the range of values of λ, denoted as the interval $[\lambda_1, \lambda_2]$, such that the corresponding ARL is not greater than a 10% of ARL; that is, for $\lambda \in [\lambda_1, \lambda_2]$, that is ARL($\lambda, h, \tau$) $\leq$ 1.1$\times$ARL(λ^*, h^*, τ) for all λ in $[\lambda_1, \lambda_2]$. For instance, if $\tau = 1.3$ then it is possible to obtain an $ARL \in [10.52, 11.57]$ for $\lambda \in [0.005, 0.5703]$. On the other hand, if $\lambda = 0.15$, it possible to obtain acceptable values of ARL (with a difference lower than 10% of ARL^*) for small shifts from $\tau \approx 1.1$ up to $\tau \approx 1.5$; if $\lambda = 0.7$, it is possible to obtain acceptable values of ARL for $\tau \geq 1.4$. We can also see that, when the shift is small, for instance, $\tau \in (1, 1.4]$, it can be noticed that

5

the differences between the ARL^* and $1.1 \times ARL^*$ are notable and therefore the variation of λ has large influence in the ARL. Conversely, for $\tau \geq 1.5$, the influence of λ in ARL is small.
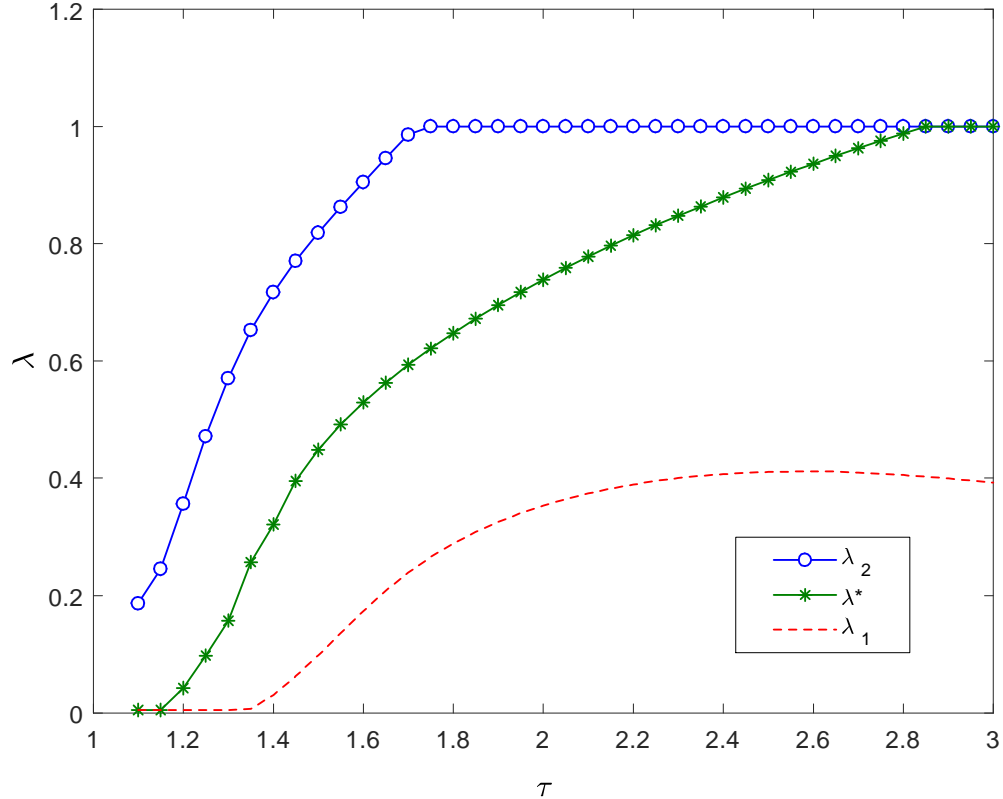

Figure 1: Relationship between the optimal λ and the range defined by λ_1 and λ_2 with the shift. The values λ_1 and λ_2 lead to an ARL of value $1.1ARL^*$.

As a conclusion, if we want an EWMA-S^2 with a good performance for all shifts, we need to use a time varying λ, that is $\lambda = \lambda_t$. The above results suggest that λ_t must depend on the shift. But, it is known that in real situations, the shift is unknown and we need to find measures of the evidence of shift based on the data. Those measures will be convert to an appropriate value λ_t. If data suggest that the process dispersion could have shifted, the value of λ_t would increase to allow y_t to be closer to the new variance. This situation would facilitate to trigger the alarm. In the other hand, if data show low evidence of being shifting, a lower value would be fixed to the parameter λ_t. This situation would facilitate the detection of a possible small shift.

In this regard, Capizzi and Masarotto (2003) propose an adaptive EWMA control chart (AEWMA) based on the behavior of data for monitoring the process mean. Later, and following the work of Crowder and Hamilton (1992) and Capizzi and Masarotto (2003), Shu (2008) presents an adaptive

τ	λ^*	**ARL***	$1.1 * \mathbf{ARL}^*$	$[\lambda_1, \lambda_2]$
1.1	0.005	41.98	46.18	[0.005, 0.187]
1.2	0.042	18.09	19.90	[0.005, 0.356]
1.3	0.157	10.52	11.57	[0.005, 0.570]
1.4	0.321	7.08	7.78	[0.030, 0.717]
1.5	0.449	5.18	5.70	[0.098, 0.819]
1.6	0.529	4.04	4.45	[0.173, 0.905]
1.7	0.593	3.31	3.64	[0.239, 0.986]
1.8	0.648	2.80	3.08	[0.289, 1.000]
1.9	0.696	2.44	2.69	[0.326, 1.000]
2.0	0.739	2.17	2.39	[0.354, 1.000]
2.1	0.778	1.97	2.17	[0.374, 1.000]
2.2	0.814	1.81	1.99	[0.389, 1.000]
2.3	0.848	1.68	1.85	[0.400, 1.000]
2.4	0.879	1.58	1.74	[0.407, 1.000]
2.5	0.909	1.50	1.65	[0.410, 1.000]
2.6	0.937	1.43	1.57	[0.411, 1.000]
2.7	0.963	1.37	1.51	[0.409, 1.000]
2.8	0.988	1.32	1.46	[0.405, 1.000]
2.9	1.000	1.28	1.41	[0.399, 1.000]
3.0	1.000	1.25	1.38	[0.392, 1.000]

Table 1: Minimum ARL for each shift τ and the corresponding λ .

EWMA control chart for monitoring increases in the process variance (AEWMA-S^2) which considers the following statistic

$$y_t = \max\left[0, y_{t-1} + \phi\left(e_t\right)\right], \quad y_0 = 0, \tag{5}$$

where, $e_t = M_t - y_{t-1}$, M_t is defined in (1) and $\phi\left(e_t\right)$ is a score function based on Huber function (Huber, 1981),

$$\phi\left(e\right) = \begin{cases} e + (1-\lambda)\gamma & \text{if } e < -\gamma \\ \lambda e & \text{if } |e| \leq \gamma \\ e - (1-\lambda)\gamma & \text{if } e > \gamma \end{cases}, \tag{6}$$

where, γ is an additional parameter of the chart. Indeed, a signal of upward shift is issued when $y_t > h$, where h is a threshold that determines the ARL$_0$. A similar procedure could be followed if we are interested in monitoring decreases in the process variance.

In this article we will analyze alternative strategies to obtain AEWMA-S^2 control charts using time-varying smoothing parameters, based on Ugaz et al. (2017), for monitoring increases in the process variance using the statistic,

$$y_t = \max\left[0, \lambda_t M_t + (1-\lambda_t) y_{t-1}\right], \quad y_0 = 0, \tag{7}$$

where, M_t is the transformed variable used by Crowder and Hamilton (1992). The alarm is triggered as soon as $y_t > h$, where h is a threshold that determines the ARL_0. Three alternative measures of a potential shift are analyzed. With these measures, we build four AEWMA-S^2 charts. The first measure of potential shift is based on the distance between the last observation M_t and the target μ_{M_t}. The second measure is based on the distance between the last observation M_t and the previous value of the control statistics y_{t-1}, as in Shu (2008). Finally, the third measure of potential shift is based only on the value of y_{t-1}. For each case, alternative score functions to convert each measure into a time-varying smoothing parameter are also used just like in Ugaz et al. (2017). In each case, procedures to compute the ARL and to optimise the charts based on Markov chain approximations are proposed.

3 AEWMA-S^2 charts with λ_t based on the last M_t

In this section, we present several proposals for measuring the evidence of the shift in the process variance based on the last transformed variable M_t. The first proposal, denoted as AEWMA1-S^2, is based on the standardized distance from M_t to the target μ_{M0}. The second proposal, denoted as AEWMA2-S^2, is based on the standardized distance from M_t to the last value of the monitoring statistics, y_{t-1}. And finally, the third proposal is a combination of the previous proposals and it is denoted by AEWMA3-S^2. Then, the smoothing parameter λ_t is obtained by using a transformation of those three distances.

3.1 The AEWMA1-S^2 chart

This adaptive control chart uses the following statistic

$$T_{1t} = \left(\frac{M_t - \mu_{M0}}{\sigma_M} \right)^2 \tag{8}$$

as a measure of the evidence of the shift. Notice that T_{1t} is the standardized distance from the last transformed variable M_t to the target μ_{M0} and it tends to be larger in presence of a shift in the process variance. The terms μ_{M0} and σ_M are obtained by the expressions (2) and (3) when $\tau = 1$. Given y_{t-1}, the value of M_t is a random variable and it is approximately normal distributed (Shu and Jiang, 2008). Therefore, if the process is in control, it holds that T_{1t} follows approximately a central chi-square distribution of one degree of freedom, χ_1^2. The cumulative distribution function is given by,

$$F_{1t} = P\left(\chi_1^2 \le T_{1t} \right). \tag{9}$$

Although F_{1t} is a natural choice for λ_t since $F_{1t} \in [0,1]$ and it is an increasing function on T_{1t}, Sánchez (2006) has shown that the variability of F_{1t} can be very large, provoking a large variance of

the monitoring statistics y_t. Then, some efficient transformation that translate F_{1t} into a smoothing parameter λ_t are required. In Ugaz et al. (2017), the following transformations have been explored:

- Linear bounded transformation

$$\lambda_{1t}^{(1)} = \lambda_{\min} + (\lambda_{\max} - \lambda_{\min}) F_{1t}, \tag{10}$$

  where $\lambda_{\min}$ and $\lambda_{\max}$ are parameters that are optimized to attain the lowest ARL for a given ARL_0, and computed with a procedure described in subsection 3.4.

- Power transformation

$$\lambda_{1t}^{(2)} = \lambda_{\min} + (\lambda_{\max} - \lambda_{\min}) F_{1t}^a, \tag{11}$$

  where a is another parameter to be optimized together with $\lambda_{\min}$ and $\lambda_{\max}$.

- Threshold transformation

$$
\begin{aligned}
\lambda_{1t}^{(3)} &= \lambda_{\min} + (\lambda_{\max} - \lambda_{\min}) q_{1t}, \\
q_{1t} &= \begin{cases} 0 & \text{if} \quad F_{1t}^a \leq p_0, \\ \dfrac{F_{1t}^a - p_0}{1 - p_0} & \text{otherwise}, \end{cases}
\end{aligned} \tag{12}
$$

  where the threshold p_0 is a constant to be optimized together with a, $\lambda_{\min}$, and $\lambda_{\max}$.

It could be noticed that $\lambda_t = \lambda_{\min}$ when F_{1t}^a is smaller than prespecified threshold, p_0 (an per-centile). Consequently, we will maintain a low smoothing factor unless the evidence of shift is large. If $F_{1t} > p_0$, we maintain a similar transformation as in (11) in such a way that the whole transformation is continuous. Moreover, the power transformation is a particular case of the threshold transformation when $p_0 = 0$, and the linear bounded transformation is a particular case of the power transformation when $a = 1$.

3.2 The AEWMA2-S^2 chart

This adaptive control chart uses the following statistic

$$T_{2t} = \left(\frac{M_t - y_{t-1}}{\sigma_M} \right)^2 \tag{13}$$

as a measure of the evidence of the shift. Notice that T_{2t} is difference between the current M_t and the value of the AEWMA statistic in the previous time, y_{t-1} and it tends to be larger in presence of a shift in the process variance. This statistic holds that

$$T_{2t} = \left(\frac{M_t - \mu_{M0}}{\sigma_M} + \frac{\mu_{M0} - y_{t-1}}{\sigma_M} \right)^2 = \left(Z_t + \frac{\mu_{M0} - y_{t-1}}{\sigma_M} \right)^2, \tag{14}$$

where Z_t is approximately a standard normal random variable (see Shu and Jiang, 2008). Given y_{t-1}, T_{2t} could be approximated by a non-central chi-square distribution of one degree of freedom, $\chi_1^2(\gamma_t)$, with noncentrality parameter $\gamma_t = (\mu_{M0} - y_{t-1})/\sigma_M$. As mentioned in Ugaz et al. (2016), the noncentrality parameter, γ_t, can be neglected for practical purposes. Thus, for the sake of simplicity, the transformation of T_{2t} into a smoothing parameter will be done by,

$$
\begin{aligned}
\lambda_{2t} &= \lambda_{\min} + (\lambda_{\max} - \lambda_{\min})\, q_{2t}, \\
q_{2t} &= \begin{cases} 0 & \text{if } G_{2t}^a \leq p_0, \\ \dfrac{G_{2t}^a - p_0}{1 - p_0} & \text{otherwise}, \end{cases} \\
G_{2t} &= P(\chi_1^2 \leq T_{2t}),
\end{aligned}
\tag{15}
$$

where the parameters $\lambda_{\min}$, $\lambda_{\max}$, p_0, and a, are optimized to minimize the ARL when the process is out of control, for a given ARL_0 using the procedure shown in subsection 3.4.

3.3   The AEWMA3-S^2 chart

This chart is a combination of the AEWMA1-S^2 and AEWMA2-S^2 charts in the sense that we consider the statistic T_{1t} or T_{2t}, which is more pessimistic with respect to the evidence of misadjustment, that is $T_{3t} = \max(T_{1t}, T_{2t})$. Consequently, the AEWMA3-S^2 chart uses the following time-varying smoothing parameter,

$$
\lambda_{3t} = \max(\lambda_{1t}^{(3)}, \lambda_{2t}),
\tag{16}
$$

which corresponds to use the statistic T_{3t} in the transformation (15).

4   AEWMA-S^2 chart based on the value of the control statistics

In this AEWMA-S^2 chart, denoted as AEWMA4-S^2, λ_t is based on the value of y_{t-1}. It uses the following statistic

$$
D_t = \left|\frac{y_{t-1}}{H}\right| = \left|\frac{y_{t-1}}{h}\right|,
$$

which is the ratio between y_{t-1} and the control limit $H = h$. The closer y_{t-1} is to the control limit, the closer D_t to 1 is. Then, using (12) with $F_{1t} = D_t$ or (15) with $G_{2t} = D_t$, the misadjustment can be converted into a time-varying smoothing parameter λ_t. It should be noticed that statistic D_t does not depend on M_t, which makes easier the ARL calculation.

5 Computation of the ARL by using a Markov chain approach

This section presents a procedure to compute the ARL of the AEWMA1-S^2, AEWMA2-S^2, and AEWMA3-S^2 charts using a Markov chain approach. Following the idea of Brook and Evans (1972), Lucas and Saccucci (1990), Capizzi and Masarotto (2003) or Shu (2008), we can approximate the value of ARL by discretizing the infinite-state transition probability matrix of the continuous-state Markov chain defined by (7). For convenience, we rewrite the control statistics of the AEWMA-S^2 as,

$$y_t = \max\left[0, y_{t-1} + (M_t - y_{t-1})\lambda_t\right]. \tag{17}$$

The procedure consists in dividing the interval $[0,h]$ in an odd number m of subintervals Ω_j, $j = 1, 2, ..., m$. These subintervals have width $\omega = (2h)/(2m-1)$, except the first subinterval whose width is $\omega/2$. Each subinterval Ω_j, that represents the $j-$th state, has as midpoint $\nu_j = (j-1)\omega$. The control statistic y_t is considered to be in the transient state or subinterval Ω_j, at time t, if $\nu_j - \omega/2 < y_t < \nu_j + \omega/2$. Furthermore, y_t falls in an absorbing state when it exceeds a threshold h. Let $P(j,k)$ be the transition probability of y_t of going from state j to state k. Then, for $j = 1, 2, 3, ...,$ m and $k \neq 1$,

$$\begin{aligned} P(j,k) &= \Pr(y_t \in \Omega_k \mid y_{t-1} \in \Omega_j) \tag{18}\\ &= \Pr(v_k - \omega/2 < y_t \leq v_k + \omega/2 \mid y_{t-1} = v_j)\\ &= \Pr((k-1)\omega - \omega/2 < v_j + (M_t - v_j)\lambda_t \leq (k-1)\omega + \omega/2)\\ &= \Pr((k-1)\omega - \omega/2 - (j-1)\omega < (M_t - v_j)\lambda_t \leq (k-1)\omega + \omega/2 - (j-1)\omega)\\ &= \Pr((k-j-1/2)\omega < (M_t - v_j)\lambda_t \leq (k-j+1/2)\omega). \tag{19} \end{aligned}$$

Let denote $a_1 = (k-j-1/2)\omega$ and $a_2 = (k-j+1/2)\omega$. Then,

$$\begin{aligned} P(j,k) &= \Pr\left[\exp(a_1) < \exp\left[\lambda_t(M_t - v_j)\right] \leq \exp(a_2)\right]\\ &= \Pr\left[\exp(a_1) < \frac{\exp(\lambda_t M_t)}{\exp(\lambda_t v_j)} \leq \exp(a_2)\right]. \tag{20} \end{aligned}$$

Note that when $k = 1$,

$$P(j,1) = \Pr\left[\frac{\exp(\lambda_t M_t)}{\exp(\lambda_t v_j)} \leq \exp(a_2)\right].$$

Replacing $M_t = \ln\left(S_t^2/\sigma_0^2\right)$ in (20),

$$\begin{aligned} P(j,k) &= \Pr\left[\exp(a_1) < \frac{\exp\left[\lambda_t \ln\left(S_t^2/\sigma_0^2\right)\right]}{\exp(\lambda_t v_j)} \leq \exp(a_2)\right]\\ &= \Pr\left[\exp(a_1) < \frac{\left(S_t^2/\sigma_0^2\right)^{\lambda_t}}{\exp(\lambda_t v_j)} \leq \exp(a_2)\right]. \tag{21} \end{aligned}$$

In the next subsections we develop procedures to calculate $P(j,k)$ for the AEWMA1-S^2 to AEWMA4-S^2 charts.

5.1 Computation of ARL of AEWMA1-S^2 to AEWMA3-S^2 charts

In the AEWMA1-S^2 to AEWMA3-S^2 charts, the expression $\left(S_t^2/\sigma_0^2\right)^{\lambda_t}/\exp\left(\lambda_t v_j\right)$ in (21) does not have a trivial distribution since λ_t depends on $\left(S_t^2/\sigma_0^2\right)$ by (12), (15) or (16). Therefore, an approximation to the distribution is proposed. In this regard, it is known that $S_t^2/\sigma_0^2 \sim \Gamma\left((n-1)/2, 2\sigma^2/\left[(n-1)\sigma_0^2\right]\right)$. Let σ_S be the standard deviation of the random variable S_t^2/σ_0^2, then, it is known that,

$$\sigma_S = \left([(n-1)/2]\left[2\sigma^2/\left[(n-1)\sigma_0^2\right]\right]^2\right)^{1/2}. \tag{22}$$

Based on (22), a suitable probability interval for S_t^2/σ_0^2 is defined, for example, $(0, 7\sigma_S]$, since probability of falling above $7\sigma_S$ is close to zero. The mentioned interval is discretized in m^* subintervals Ψ_i, $i = 1, 2, 3, ..., m^*$. Similarly to the previous discretization, the width of the subintervals is defined by $\varepsilon = 7\sigma_S/(2m^*-1)$ and the midpoint of i−th subinterval Ψ_i is denoted by u_i. If $S_t^2/\sigma_0^2 \in \Psi_i$ then $u_i - \varepsilon/2 < S_t^2/\sigma_0^2 \le u_i + \varepsilon/2$. In each of these subintervals, we approximate S_t^2/σ_0^2 to the value u_i. The approximate values for S_t^2/σ_0^2 can be used to assign an approximate value to M_t and λ_t in each subinterval as,

$$T_{1t} \approx \left(\frac{\ln u_i - \mu_{M0}}{\sigma_M}\right)^2 \equiv c_i \;\; \text{or} \;\; T_{2t} \approx \left(\frac{\ln u_i - v_j}{\sigma_M}\right)^2 \equiv c_i \;\; \text{or} \;\; T_{3t} \approx \max\left(T_{1t}, T_{2t}\right) \equiv c_i$$

$$r_i = P\left(\chi_1^2 < c_i\right)$$

$$q_i = \begin{cases} 0 & \text{if} \quad r_i^a \le p_0, \\ \dfrac{r_i^a - p_0}{1 - p_0} & \text{otherwise}, \end{cases}$$

$$\lambda_i = \lambda_{\min} + \left(\lambda_{\max} - \lambda_{\min}\right) q_i.$$

In consequence, if we want to approximate the values of $P(j, k)$ in (18), we can condition on each subinterval Ψ_i and apply the total probability formula as,

$$
\begin{aligned}
P(j, k) &= \Pr\left[\exp(a_1) \le \frac{\left(S_t^2/\sigma_0^2\right)^{\lambda_t}}{\exp\left(\lambda_t v_j\right)} \le \exp(a_2)\right] \\
&= \sum_{i=1}^{m} \Pr\left[\exp(a_1) \le \frac{\left(S_t^2/\sigma_0^2\right)^{\lambda_t}}{\exp\left(\lambda_t v_j\right)} \le \exp(a_2) \;\middle|\; S_t^2/\sigma_0^2 \in \Psi_i\right] \Pr\left[S_t^2/\sigma_0^2 \in \Psi_i\right] \\
&\approx \sum_{i=1}^{m} \Pr\left[\exp(a_1) \le \frac{\left(u_i\right)^{\lambda_i}}{\exp\left(\lambda_i v_j\right)} \le \exp(a_2)\right] \Pr\left[S_t^2/\sigma_0^2 \in \Psi_i\right].
\end{aligned}
\tag{23}
$$

Notice that since u_i is a constant in each subinterval, the first probability at the right hand side of (23) is easy to compute, since it is just 1 or 0. The second one is also easy to compute, since we have that $S_t^2/\sigma_0^2 \sim \Gamma\left((n-1)/2, 2\sigma^2/\left[(n-1)\sigma_0^2\right]\right)$. Finally, let $\mathbf{R}_{m \times m}$ be a submatrix that contains the probabilities $P(j, k)$ of going from the transient state j to the state k, $\mathbf{p}_{ini}$ is an initial probability

vector of the states, $\mathbf{I}$ is the $m \times m$ identity matrix, and $\mathbf{1}$ is a $m \times 1$ vector of ones. Then, the probability function of RL and hence the ARL in zero-state (ARL^{ZS}), are given by,

$$\Pr\left(RL = rl\right) = \mathbf{p}'_{ini}\left(\mathbf{R}^{rl-1} - \mathbf{R}^t\right)\mathbf{1},$$

and

$$\text{ARL}^{ZS} = \mathbf{p}'_{ini}\left(\mathbf{I} - \mathbf{R}\right)^{-1}\mathbf{1}, \tag{24}$$

respectively.

Lucas and Saccucci (1990) or Shu (2008) suggest using the cyclic probability steady-state vector, $\mathbf{p}_{ss}$, for calculating the ARL in steady-state (ARL^{SS}). The $\mathbf{p}_{ss}$ vector is obtained by solving $\mathbf{p}_{ss} = \mathbf{P}'_1\mathbf{p}_{ss}$, subject to $\mathbf{1}'\mathbf{p}_{ss} = 1$, where $\mathbf{P}_1$ is the ergodic transition probability matrix defined by,

$$\mathbf{P}_1 = \begin{pmatrix} \mathbf{R} & (\mathbf{I} - \mathbf{R})\mathbf{1} \\ \mathbf{e}'_1 & 0 \end{pmatrix},$$

where $\mathbf{e}'_1 = (1\ 0\ 0...0)$. Hence, the ARL^{SS} is obtained by,

$$\text{ARL}^{SS} = \mathbf{q}'\left(\mathbf{I} - \mathbf{R}\right)^{-1}\mathbf{1}, \tag{25}$$

where, $\mathbf{q}$ is a vector of length m obtained from $\mathbf{p}_{ss}$ by deleting the entry corresponding to the absorbing state and normalizing so that the probabilities sum to 1.

5.2 Computation of ARL of AEWMA4-S^2 charts

For the AEWMA4-S^2 chart, λ_t does not depend on M_t. The computation of the ARL follows the traditional procedure proposed by Brook and Evans (1972) and Lucas and Saccucci (1990). The transition probability defined in (19) can be reexpressed as follows

$$
\begin{aligned}
P\left(j,k\right) &= \Pr\left[\nu_k - \nu_j - \omega/2 \le \left(M_t - \nu_j\right)\lambda_t \le \nu_k - \nu_j + \omega/2\right] \\
&= \Pr\left[\frac{\nu_k - \nu_j - \omega/2}{\lambda_t} - \nu_j \le M_t \le \frac{\nu_k - \nu_j + \omega/2}{\lambda_t} - \nu_j\right] \\
&= \Pr\left[\exp\left(b_1\right) < \exp\left(M_t\right) \le \exp\left(b_2\right)\right] \\
&= \Pr\left[\exp\left(b_1\right) < S_t^2/\sigma_0^2 \le \exp\left(b_2\right)\right],
\end{aligned}
\tag{26}
$$

where, $b_1 = \left(\nu_k - \nu_j - \omega/2\right)/\lambda_t - \nu_j$, $b_2 = \left(\nu_k - \nu_j + \omega/2\right)/\lambda_t - \nu_j$. The probability (26) is computed using that $S_t^2/\sigma_0^2 \sim \Gamma\left((n-1)/2, 2\sigma^2/\left[(n-1)\sigma_0^2\right]\right)$. The ARL^{ZS} o ARL^{SS} are calculated by (24) and (25), respectively.

5.3   Optimisation of parameters

It is important to note that it is considering a process $X_t \approx N(\mu_0, \tau^2 \sigma^2)$. Let $\beta = (\lambda_{\min}, \lambda_{\max}, p_0, a, h)$ be the parameters that define the AEWMA-S^2 chart, and let $\mathrm{ARL}^{ZS}(\tau, \beta)$ be the ARL of a scheme with parameters equal to β and shift τ. Let ARL_0^{ZS} be the in-control ARL. In order to evaluate the performance of an AEWMA-S^2 chart in a set of shifts $\boldsymbol{\tau} = (\tau_1, ..., \tau_k)$ we need to define a function f $(\beta, \boldsymbol{\tau}) : \mathbb{R}^k \to \mathbb{R}$, which summarises the overall performance of the chart along the alternative shifts $\boldsymbol{\tau}$. This function will be minimised when the optimal parameters β^* are used. That is, β^* is the solution of the following optimisation problem:

$$\min_\beta f \ (\beta, \boldsymbol{\tau}).$$

subject to: (27)

$$\mathrm{ARL}^{ZS}(1, \beta) = \mathrm{ARL}_0^{ZS},$$

Here, we use the weighted Euclidean distance to define the function f $(\beta, \boldsymbol{\tau})$:

$$f \ (\beta, \boldsymbol{\tau}) = \sum_{i=1}^{k} \omega_i \left(ARL^{ZS}(\tau_i, \beta) - ARL^*(\tau_i) \right)^2, \tag{28}$$

where $ARL^*(\tau_i)$ is the minimum ARL for shift τ_i attained using the optimal EWMA-S^2 chart, as shown in Table 1. This function is simple and has good performance. Besides, it allows us to specialise the chart over some range of values in which we are more interested. Of course, other choises for f $(\beta, \boldsymbol{\tau})$ can be used, for instance, f $(\beta, \boldsymbol{\tau}) = \sum\limits_{i=1}^{k} ARL^{ZS}(\tau_i, \beta).$

Table 2 shows the optimal values β^* for $ARL_0^{ZS} = 200$ based on (27) and (28) with rational subgroup of size $n = 5$. For each value of ARL_0^{ZS} two different designs are proposed and compared. In the first, the optimisation (27) is based on the range of shifts $\tau \in [1.1, 2]$, where (28) uses higher weights on the extremes of this interval. By doing so, we want to assure good sensitivity to small shifts, without losing efficiency at large shifts. The resulting charts are denoted as AEWMA-S^2-1: AEWMA1-S^2-1, AEWMA2-S^2-1, AEWMA3-S^2-1 and AEWMA4-S^2-1, respectively. In the second design, the optimisation (27) is based on the range of shifts $\tau \in [1.4, 2]$, where (28) again uses higher weights on the extremes of this interval. In this case, we want to assure good performance at moderate and large shifts. The resulting charts are denoted as AEWMA-S^2-2: AEWMA1-S^2-2, AEWMA2-S^2-2, AEWMA3-S^2-2 and AEWMA4-S^2-2, respectively. For simplicity, and without any loss of generality, $\mu_0 = 0$ and $\sigma = 1$ is assumed.

β^*	ARL$_0^{ZS}$=200					ARL$_0^{SS}$=200				
	λ_{min}^*	λ_{max}^*	a^*	p_0^*	h^*	λ_{min}^*	λ_{max}^*	a^*	p_0^*	h^*
					Panel A					
AEWMA1-S^2-1	0.0632	0.1115	2.3458	0.3584	0.2225	0.0181	0.2249	7.5594	0.8866	0.0546
AEWMA2-S^2-1	0.0277	0.0787	4.0097	0.0278	0.1188	0.0145	0.7524	7.2188	0.7570	0.0445
AEWMA3-S^2-1	0.0769	0.1399	8.5720	0.5060	0.2062	0.0385	0.2510	7.8067	0.8832	0.1085
AEWMA4-S^2-1	0.0886	0.5863	9.4988	0.9983	0.2182	0.0821	0.1121	5.1453	0.2222	0.2059
					Panel B					
AEWMA1-S^2-2	0.1888	0.6239	5.8904	0.2990	0.6812	0.1271	0.3439	3.8760	0.2403	0.5240
AEWMA2-S^2-2	0.3731	1.0000	9.3896	0.2425	0.6875	0.1770	0.3395	9.5038	0.0357	0.4029
AEWMA3-S^2-2	0.2441	0.6578	4.3676	0.3361	0.7717	0.1527	0.2843	3.1404	0.5305	0.4165
AEWMA4-S^2-2	0.5644	0.6644	1.1987	0.8917	0.8373	0.2377	0.4377	10.9715	0.9900	0.4589

Table 2: Optimal parameters of the AEWMA-S^2 control charts. Panel A: parameters optimised for the range $\tau \in [1.1, 2]$. Panel B: parameters optimised for the range $\tau \in [1.4, 2]$.

6   Comparisons

In this section, the four proposed AEWMA-S^2 control charts are compared. Besides, they are compared to other control charts such as Shewhart-S^2 control chart, the EWMA-S^2 control charts, the EWMA-S^2 of Castagliola et al (2010) called here EWMA-S^2-CT and the adaptive EWMA control charts for the variance of Shu (2008) called here AEWMA-S^2-SH. Unless otherwise stated, all the comparisons were made using: zero-state ARL, $ARL_0 = 200$ and $n = 5$.

Table 3 shows that the performance of the four proposed AEWMA-S^2-1 charts are similar for small and medium shifts, in the range $(1, 1.4]$. However, the AEWMA1-S^2-1 design shows a slightly better performance than the others in approximately the interval $(1, 1.2]$. In the interval of shifts $(1.2, 3]$, the AEWMA2-S^2-1 shows the better performance and followed by AEWMA3-S^2-1 y 1-S^2-1. The AEWMA4-S^2-1 design loses efficiency for medium and large shifts.

On the other hand, Table 3 shows that also the four AEWMA-S^2-2 designs have similar performance for small and medium shifts in the variance process, approximately $(1, 1.5]$. In that range, it can be seen the AEWMA1-S^2-2 is the best one. In the interval of shifts $\tau \in (1.5, 3]$, the AEWMA2-S^2-2 design shows the better performance. The AEWMA4-S^2-2 design loses efficiency for medium and large shifts.

In Table 3, we can compare the four AEWMA-S^2-1 designs and a Shewhart-S^2 control chart with the same rational subgroup size, $n = 5$ (S-1 design). It can be seen that Shewhart control chart is not competitive for small and medium shifts, even up to $\tau < 2$. Also, we can compare the four AEWMA-S^2-2 charts and the same Shewhart-S^2 design (S-1). In this case, S-1 is still less competitive than four AEWMA-S^2-2 designs for $\tau < 3$.

Besides, we can compare the ARL values of the four AEWMA-S^2-1 designs and two alternative EWMA-S^2 designs. These EWMA-S^2 charts are designed to get minimum ARL values at shifts $\tau = 1.1$ (E-1) and $\tau = 1.5$ (E-2). In this case, it can be seen that the four proposed AEWMA-S^2 designs and only E-1 have a similar performance for small shifts, the AEWMA1-S^2-1 is the best one. E-1 is only competitive in $\tau = 1.1$. E-2 is not competitive for small and medium shifts, up to $\tau = 1.3$. For $\tau = 1.4$, the first three AEWMA-S-1 charts are better than E-2, even the AEWMA2-S^2-1 up to $\tau = 1.5$. For large shifts, approximately $\tau > 1.5$, the first three AEWMA-S^2-1 designs are competitive with E-2 but E-1 is not competitive. Definitely, the four proposed AEWMA-S^2-1 control charts show good performance through the whole shifts range. Additionally, we can compare the ARL values of the second four AEWMA-S^2-2 charts and the EWMA-S^2 with designs that were obtained for minimum ARL values at shifts $\tau = 2$ (E-3) and $\tau = 3$ (E-4). In this case, it can be seen that the four proposed AEWMA-S^2 designs have good performance up to $\tau \leq 2$. E-3 is competitive only for $\tau > 2$ and E-4 for $\tau \geq 2.5$. Note that for $\tau = 2$, the first three designs have a good behavior and AEWMA2-S^2-2 is the best one, even up to $\tau = 3$.

Moreover, Table 3 allows us to compare the ARL values of the four AEWMA-S^2-1 designs with two alternative EWMA-S^2-CT charts. These EWMA-S^2-CT charts are designed to get minimum ARL values at shifts $\tau = 1.1$ (CT-1) and $\tau = 1.5$ (CT-2). This comparison shows that the four proposed AEWMA-S^2-1 control charts are more competitive than CT-1 for the whole range of shifts. For small an medium shifts, $\tau < 4$, the four proposals are more competitive than CT-2. Furthermore, we can compare the ARL values of the four AEWMA-S^2-2 charts and the EWMA-S^2-CT charts for two design, with minimum ARL values at shifts $\tau = 2$ (CT-3) and $\tau = 3$ (CT-4). In this case, it can be seen that the four proposed AEWMA-S^2 control charts have a competitive performance for all shift, CT-3 and CT-4 are only competitive for $\tau \geq 2.5$.

Our final comparison is between the proposed AEWMA-S^2 control charts and the AEWMA-S^2 control charts of Shu (2008). In this regard, Table 3 allows us to compare the four proposed AEWMA-S^2-1 control charts (designs optimized for $\tau \in [1.1, 2]$ as in Shu, 2008) with the AEWMA-S^2-SH-1 (design optimized for $\tau \in [1.1, 2]$). This design is labelled as SH-1. The first three proposed AEWMA-S^2-1 are better than SH-1 for small and medium shifts, approximately for $\tau \in [1.1, 1.2]$, where the AEWMA1-S^2-1 is the best one. In the interval $\tau \in (1.2, 1.4]$, the first three AEWMA-S^2-1 control charts are better than the AEWMA-S^2-SH-1, where, the AEWMA2-S^2-1 is the most competitive. Then, in general, for large shifts, these designs are similar, being AEWMA4-S^2-1 less competitive. It is worth mentioning that, in the range $\tau \in (1.4, 1.7]$, the AEWMA2-S^2-1 and 3-S^2-1 are more efficient than SH-1, where, AEWMA2-S^2-1 is the most competitive.

$ARL_0^{ZS}=200$	τ									
	1.1	**1.2**	**1.3**	**1.4**	**1.5**	**1.6**	**1.7**	**2.0**	**2.5**	**3.0**
1-S²-1	**41.79**	**17.19**	10.04	7.01	5.40	4.43	3.78	2.71	1.95	1.58
2-S²-1	41.99	17.20	**9.91**	**6.82**	5.18	4.18	3.52	2.43	1.70	1.39
3-S²-1	42.63	17.41	10.00	6.87	5.22	4.22	3.55	2.45	1.71	1.40
4-S²-1	43.96	18.19	10.60	7.41	5.74	4.74	4.08	3.00	2.25	1.87
1-S²-2	53.09	21.14	11.22	7.16	**5.14**	3.99	3.26	2.16	1.51	1.27
2-S²-2	54.44	21.74	11.43	7.22	5.15	**3.97**	**3.23**	**2.14**	1.50	1.26
3-S²-2	54.19	21.73	11.47	7.26	5.18	3.99	3.26	2.15	1.51	1.27
4-S²-2	53.85	21.78	11.56	7.33	5.23	4.05	3.31	2.21	1.55	1.30
S-1	95.15	42.39	21.58	12.61	8.24	5.86	4.46	2.55	1.61	1.30
E-1	41.98	18.19	11.13	8.06	6.40	5.37	4.67	3.48	2.64	2.26
E-2	51.41	20.64	11.07	7.14	5.18	4.06	3.35	2.29	1.62	1.34
E-3	58.11	24.00	12.64	7.87	5.50	4.17	3.36	2.17	1.51	1.27
E-4	65.03	28.27	15.04	9.25	6.32	4.67	3.66	2.24	1.50	**1.25**
CT-1	46.33	20.64	13.17	9.73	7.76	6.48	5.58	3.96	2.67	2.03
CT-2	58.98	22.47	11.66	7.39	5.30	4.13	3.39	2.28	1.60	1.33
CT-3	60.70	24.91	12.99	8.02	5.57	4.20	3.36	2.16	1.49	1.26
CT-4	65.02	28.27	15.04	9.25	6.32	4.67	3.66	2.24	1.50	1.25
SH-1	44.37	18.20	10.48	7.17	5.39	4.29	3.55	2.35	1.59	1.30
SH-2	56.41	22.63	11.81	7.40	5.23	4.01	3.26	**2.14**	**1.49**	**1.25**

Table 3: ARL in zero state comparison between competing control charts for $ARL_0 = 200$ and $n = 5$. The following charts are considered (Abbreviations for each chart appear in parentheses): AEWMA1-S²-1 (1-S²-1), AEWMA2-S²-1 (2-S²-1), AEWMA3-S²-1 (3-S²-1), AEWMA4-S²-1 (4-S²-1), AEWMA1-S²-2 (1-S²-2), AEWMA2-S²-2 (2-S²-2), AEWMA3-S²-2 (3-S²-2), AEWMA4-S²-2 (4-S²-2), Shewhart-S² (S-1), EWMA-S²-1 (E-1), EWMA-S²-2 (E-2), EWMA-S²-3 (E-3), EWMA-S²-4 (E-4), EWMA-S²-CT1 (CT-1), EWMA-S²-CT2 (CT-2), EWMA-S²-CT3 (CT-3), EWMA-S²-CT4 (CT-4), AEWMA-S²-SH-1 (SH-1) and AEWMA-S²-SH-2 (SH-2). The adaptive chart with the lowest ARL at each shift is shown in bold.

Finally, in table 3 we can compare the four proposed AEWMA-S²-2 control charts (designs optimized for $\tau \in [1.4, 2]$ as it was mentioned in the previous section) with the AEWMA-S²-SH-2 (design optimized for $\tau \in [1.4, 2]$ as it was mentioned in Shu, 2008). This design is labelled as SH-2. In general, again, it can be seen that the ARL of the four proposed AEWMA-S²-2 designs and SH-2 are similar in almost all range of shifts. The four AEWMA-S²-2 proposed take advantage of SH-2 for small and medium shifts, approximately for $\tau \in (1, 1.6]$, except for the AEWMA4-S²-2 in the interval $\tau \in [1.5, 1.6]$. The AEWMA1-S²-2 is the most competitive up to $\tau = 1.5$ and the AEWMA2-S²-2 for $\tau = 1.6$. The AEWMA2-S²-2 is the most competitive for $\tau = 1.7$. It can be concluded that the proposed AEWMA-S² control chart are more competitive than the AEWMA-S²-SH in terms of ARL particularly for small and medium shifts.

7   Conclusions

We have presented four adaptive EWMA control charts for monitoring the variance of a variable that represents a quality characteristic in a particular process. These control charts work with a time varying smoothing parameter. The proposed AEWMA-S^2 control charts are very easy to understand and to implement in the practice. We should have in mind that the size shift depends on the nature of the monitored process. Since in actual operation, smaller shifts are more frequent than larger shifts, we have shown that these proposed charts have a good performance for small and medium shifts and even for large shifts. Therefore, the proposed charts can be competitive with respect to the alternative charts of the literature on a wide range of shifts.

7.0.1   Acknowledgements

References

[1] Abbasi, S. A. (2010). On sensitivity of EWMA control chart for monitoring process dispersion. In Proceedings of the World Congress on Engineering, 3, 2027-2032.

[2] Abbasi, S. A. and Miller, A. (2013). MDEWMA chart: an efficient and robust alternative to monitor process dispersion. Journal of Statistical Computation and Simulation, 83(2), 247-268.

[3] Acosta-Mejia, C. A. (1998). Monitoring reduction in variability with the range. IIE transactions, 30(6), 515-523.

[4] Acosta-Mejia, C. A., Pignatiello, J. J. and Rao, B. V. (1999). A comparison of control charting procedures for monitoring process dispersion. IIE transactions, 31(6), 569-579.

[5] Amin, R. W., Wolff, H., Besenfelder, W. and Baxley Jr, R. (1999). EWMA control charts for the smallest and largest observations. Journal of Quality Technology, 31(2), 189-201.

[6] Bagshaw, M. and Johnson, R. A. (1975). The effect of serial correlation on the performance of CUSUM tests II. Technometrics, 17(1), 73-80.

[7] Box, G. E., Hunter, W. G. and Hunter, J. S. (1978). Statistics for experimenters. John Wiley & Sons, New York, NY.

[8] Box, G. E. P. and Ramirez, J. G (1991a). Sequential Methods in Statistical Process Monitoring. Report No. 65, Center for Quality and Productivity Improvement, University of Wisconsin-Madison, Madison, WI.

[9] Box, G, E. P. and Ramirez, J. G. (1991b). Sequential Methods in Statistical Process Monitoring. Report No. 66, Center for Quality and Productivity Improvement, University of Wisconsin-Madison, Madison, WI.

[10] Box, G. E. P. and Ramirez, J. G. (1991c). Sequential Methods in Statistical Process Monitoring. Report No. 67, Center for Quality and Productivity Improvement, University of Wisconsin-Madison, Madison, WI.

[11] Brook D. and Evans D. A. (1972). An approach to the probability distribution of CUSUM run length. Biometrika, 59(3), 539-549.

[12] Capizzi G. and Masarotto G. (2003). An adaptive exponentially weighted moving average control chart. Technometrics, 45(3), 199-207.

[13] Castagliola, P. (2005). A New S2-EWMA Control Chart for Monitoring the Process Variance. Quality and Reliability Engineering International, 21(8), 781-794.

[14] Castagliola, P., Celano, G. and Fichera, S. (2009). A new CUSUM-S^2 control chart for monitoring the process variance. Journal of Quality in Maintenance Engineering, 15(4), 344-357.

[15] Castagliola, P., Celano, G. and Fichera, S. (2010). A Johnson's type transformation EWMA-S^2 control chart. International Journal of Quality Engineering and Technology, 1(3), 253-275.

[16] Chang, T. C. and Gan, F. F. (1995). Cumulative sum control chart for monitoring process variance. Journal of Quality Technology. 27(2), 109-119.

[17] Chao-Wen, L. and Reynolds Jr, M. R. (1999). Control charts for monitoring the mean and variance of autocorrelated process. Journal of Quality Technology, 31(3), 259-274.

[18] Crowder, S. V.and Hamilton, M. D. (1992). An EWMA for monitoring a process standard deviation. Journal of Quality Technology, 24(1), 12-21.

[19] Gan, F. F. (1995). Joint monitoring of process mean and variance using exponentially weighted moving average control charts. Technometrics, 37(4), 446-453.

[20] Haq, A., Brown, J. and Moltchanova, E. (2014). New exponentially weighted moving average control charts for monitoring process mean and process dispersion. Quality and Reliability Engineering International.

[21] Hawkins, D. M. (1981). A CUSUM for a scale parameter. Journal of Quality Technology, 13(4), 228-231.

[22] Huber P. J. (1981). Robust statistics. New York: Wiley.

[23] Huwang, L., Huang, C. J. and Wang, Y. H. T. (2010). New EWMA control charts for monitoring process dispersion. Computational Statistics & Data Analysis, 54(10), 2328-2342.

[24] Johnson, N. L. (1949). Systems of frequency curves generated by methods of translation. Biometrika, 36(1-2), 149-176.

[25] Lowry, C. A., Champ, C. W. and Woodall, W. H. (1995). The performance of control charts for monitoring process variation. Communications in Statistics-Simulation and Computation, 24(2), 409-437.

[26] Lucas J. M. and Saccucci M. S. (1990). Exponentially weighted moving average control schemes: Properties and Enhancements (with discussion), Technometrics, 32(1), pp. 1-29.

[27] MacGregor, J. F. and Harris, T. J. (1993). The exponentially weighted moving variance. Journal of Quality Technology, 25(2), 106-118.

[28] Maravelakis, P. E. and Castagliola, P. (2009). An EWMA chart for monitoring the process standard deviation when parameters are estimated. Computational Statistics & Data Analysis, 53(7), 2653-2664.

[29] Nazir, H. Z., Riaz, M. and Does, R. J. (2015). Robust CUSUM control charting for process dispersion. Quality and Reliability Engineering International, 31(3), 369-379.

[30] Ng, C. H. and Case, K. E. (1989). Development and evaluation of control charts using exponentially weighted moving averages. Journal of Quality Technology, 21(4), 242-250.

[31] Page, E. S. (1963). Controlling the standard deviation by CUSUMS and warning lines. Technometrics, 5(3), 307-315.

[32] Sánchez, I. (2006). Recursive estimation of dynamic models using Cook's distance, with application to wind energy forecast. Technometrics, 48(1), 61-73.

[33] Shewhart W. A. (1931). Economic control of quality of manufactured product. D. Van Nostrand Company, Inc, The United States of America, 182.

[34] Shu, L. (2008). An adaptive exponentially weighted moving average control chart for monitoring process variances. Journal of Statistical Computation and Simulation, 78(4), 367-384.

[35] Shu, L. and Jiang, W. (2008). A new EWMA chart for monitoring process dispersion. Journal of Quality Technology, 40(3), 319-331.

[36] Shu, L., Yeung, H. F. and Jiang, W. (2010). An adaptive CUSUM procedure for signaling process variance changes of unknown sizes. Journal of Quality Technology, 42(1), 69.

[37] Sparks, R. S. (2000). CUSUM Charts for Signaling Varying Location Shifts. Journal of Quality Technology 32(2), 157-171.

[38] Sweet, A. L. (1986). Control charts using coupled exponentially weighted moving averages. IIE Transactions, 18(1), 26-33.

[39] Tuprah, K. and Ncube, M. (1987). A comparison of dispersion quality control charts. Sequential Analysis, 6(2), 155-163.

[40] Ugaz, W., Sánchez, I. and Alonso, A. M. (2017). Adaptive EWMA control charts with time-varying smoothing parameter. The International Journal of Advanced Manufacturing Technology, 93(9-12), 3847-3858.

[41] Wortham, A. W. and Ringer, L. J. (1971). Control via exponential smoothing. The Logistics Review, 7(32), 33-40.

[42] Yashchin, E. (1995). Estimating the current mean of a process subject to abrupt changes. Technometrics, 37(3), 311–323.